CHALMERS
UNIVERSITY OF TECHNOLOGY

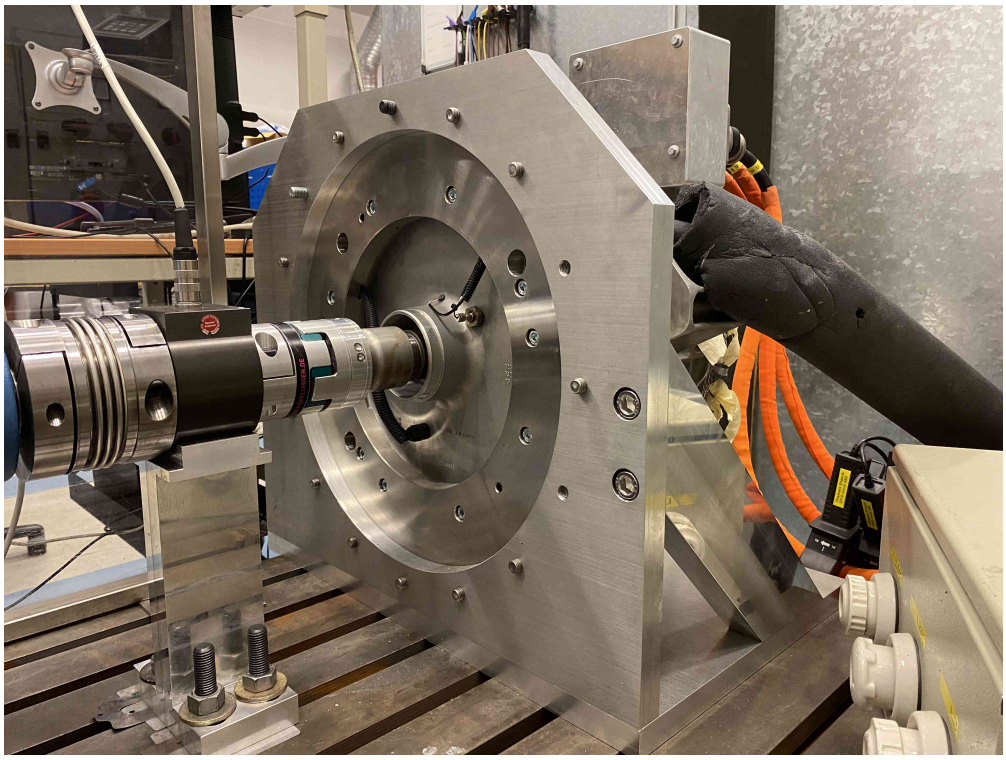

Field-oriented control of ASM - comparison between simulated and measured performance

An analysis of the differences between simulating and measuring the performance of an induction motor using volts by hertz and field-oriented control

Degree project report in Electrical Engineering

JONATHAN BLOMQWIST
ALBIN BJÖRFELT

DEPARTMENT OF ELECTRICAL ENGINEERING
CHALMERS UNIVERSITY OF TECHNOLOGY
Gothenburg, Sweden 2024
www.chalmers.se

Degree project report 2024

Field-oriented control of ASM - comparison between simulated and measured performance

An analysis of the differences between simulating and measuring the performance of an induction motor using volts by hertz and field-oriented control

JONATHAN BLOMQWIST
ALBIN BJÖRFELT

CHALMERS
UNIVERSITY OF TECHNOLOGY

Department of Electrical Engineering
Chalmers University of Technology
Gothenburg, Sweden 2024

Field-oriented control of ASM - comparison between simulated and measured performance
An analysis of the differences between simulating and measuring the performance of an induction motor using volts by hertz and field-oriented control
JONATHAN BLOMQWIST
ALBIN BJÖRFELT

Supervisor: Qixuan Wang, Department of Electrical Engineering
Supervisor: Joachim Härsjö, Volvo Cars
Examiner: Torbjörn Thiringer, Department of Electrical Engineering

Degree project report 2024
Department of Electrical Engineering
Chalmers University of Technology
SE-412 96 Gothenburg
Sweden
Telephone +46 31 772 1000

Cover: The induction machine, in the project referred to as the "large machine".

Typeset in LaTeX
Gothenburg, Sweden 2024

Field-oriented control of ASM - comparison between simulated and measured performance
An analysis of the differences between simulating and measuring the performance of an induction motor using volts by hertz and field-oriented control
JONATHAN BLOMQWIST
ALBIN BJÖRFELT
Department of Electrical Engineering
Chalmers University of Technology

Abstract

The goal of this degree project was to control an induction machine in real-time with dSPACE and to compare the performance difference between the real machine and a simulated test. The work was conducted within a larger cooperation project with Volvo Cars. The aim was to improve simulation accuracy of induction machines. The controls and the simulations for this project were created in Simulink. The performance test was carried out in a laboratory environment using dSPACE to control the machine in real time. Important findings for the control were that anti-windup was needed for the PI-regulators and that the flux strongly influenced the performance. For the performance test it was found that the reactive input power for the real machine was twice as high at no-load as for the same test in the simulation. Under load, active input power was two times greater for the simulated test compared to the measurements on the real induction machine. Torque ripple was large for the real machine but it was stable in the simulations. The reasons for the differences between the real machine and the simulations were not investigated further.

Keywords: Induction machine, Field-oriented control, V/Hz, Simulation, dSPACE, Simulink, Performance test, Real-time control

Acknowledgements

This degree project was conducted by two BSc electrical engineering students over 20 weeks and corresponds to 15 ECTS. Thanks to Meng-Ju for providing the parameters to the large machine. Thanks to Stefan for providing a lot of practical help and safety checks in the laboratory. Thanks to Douglas for providing safety checks and helping during the parameter tests of the small machine. Thanks to Qixuan for explaining how to use dspace and a lot of helpful tips during our work. Thanks to Joachim and Volvo Cars for the collaboration. Thanks to our examiner Torbjörn for giving us the chance to work with this project.

Jonathan Blomqwist and Albin Björfelt, Gothenburg, May 2024

Contents

1
Introduction

1.1 Problem background

The transition to fully electric vehicles (EVs) places great demands on the development and simulation of electric machines. Today the most widely used electric machine for electric vehicles is the permanent magnet synchronous machine (PMSM). However, the capabilities of the vehicle can be improved by introducing a second electrical machine, the asynchronous machine (AM), also called induction machine (IM). The IM and the PMSM can work great together by complementing each other. However the induction machine is lagging behind in case of simulation and modelling. It would thus be of great advantage for the improvement of EV capabilities to further investigate simulation and modelling accuracy of the IM. [1]

1.2 Purpose

The purpose of this project is to increase the simulation and modelling accuracy of induction machines. Using field-oriented control an induction machine will be tested and then simulated in Simulink. By analysing the differences in real measurements and simulated measurements the goal is to identify the underlying causes of the differences. This work can therefore help to facilitate the implementation of induction machines in the vehicle industry and other applications.

1.3 Limitations

The primary part of this project will focus on the actual creation and implementation of the IM control and conducting tests. The simulation of the machine will not be built from scratch in this project. A Simulink toolbox model for an IM will be used for the simulation.

2

Theory

2.1 Induction Machine

The IM is an asynchronous AC-machine. Unlike synchronous machines (SMs), for example the PMSM, the IM is magnetized from the stator. Through a supply of three-phase voltages to the windings in the stator a rotating electromagnetic field is created. The speed that this flux is rotating with is controlled by the supply frequency and is called the *synchronous speed* (ω_1). When the rotor is rotating at the same speed as the synchronous speed, no torque will be generated in the rotor. However, when the rotor rotates at a different speed, forces generated in the rotor windings will try to restore the rotational speed of the rotor to the synchronous speed. According to Lenz' law a current will be induced in the rotor windings if the rotor is lagging behind the synchronous speed of the stator field. A current in an electromagnetic field creates force, which gives the *electrical torque*. [2]

2.1.1 T-model

The most widely used model for the induction machine is the T-model. In this model, shown in figure 2.1, R_s represents the winding resistance of the stator. $L_{s\sigma}$ and $L_{r\sigma}$ represents the leakage inductances of the stator and rotor. L_m is the mutual inductance between the stator and the rotor. The voltage source in series with the rotor resistance R_r, is called the rotor emf. It is the rotor emf that represents the conversion from electrical power to mechanical power. [2]

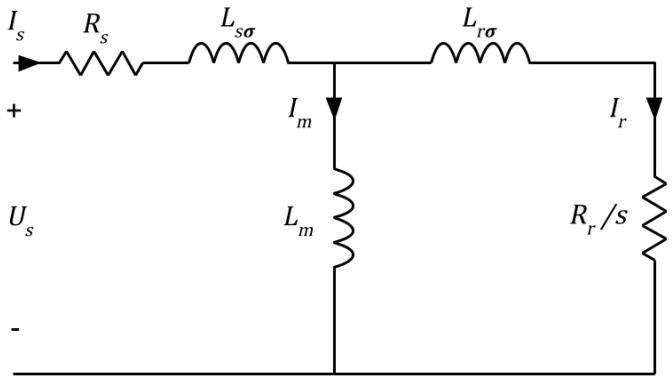

Figure 2.1: The T-model representation of an IM where U_s, I_s, I_m, I_r and s are the stator voltage, stator current, magnetising current, rotor current and the slip, respectively.

2.1.2 The Inverse-Γ model

To simplify the T-model the inverse-Γ model can be used. It has less parameters and is therefore more desirable when designing a controller for the induction machine. The inverse-Γ model is shown in figure 2.2. [2]

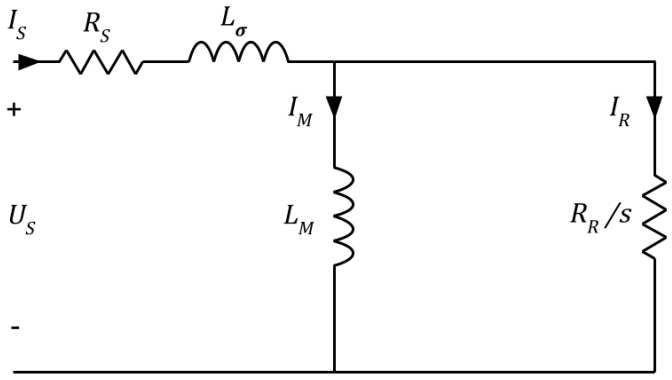

Figure 2.2: The inverse-Γ model representation of an IM where U_S, I_S, I_M and I_R are the stator voltage, stator current, magnetising current and rotor current, respectively. R_S, L_σ, L_M and R_R are the stator resistance, total leakage inductance, mutual inductance and rotor resistance denoted with capital letters to underscore that they are in inverse-Γ representation.

2.2 Transformations

2.2.1 Direct and quadrature-vector

When talking about motor control there is three different frames or "perspectives" of voltage and currents. There is the normal "real" frame in three-phase, the "alpha and beta" stationary frame in two-phase and the "direct and quadrature" rotating frame.

Due to the fact that balanced three-phase quantities always add to zero (called zero-sequence) at any given time no information is lost when transforming to a two phase system. The two phases in the stationary frame called alpha and beta can be further transformed. This is done by removing the rotation and therefore viewing the two phases as DC values instead of AC values. The two phases in this rotating frame is called direct and quadrature vectors (d and q vectors). When discussing currents in an induction motor it is preferable to align the d-current vector with the rotor flux and q-current vector shifted 90 degrees from the d-current vector. This way the rotor flux, or magnetisation of the machine, can be controlled purely by controlling the d-current. The q-current becomes a representation of the torque in the motor and can also be controlled individually. [3]

2.2.2 Clarke

The Clarke transformation is a transformation used for identifying the real and imaginary part of a current or voltage. In this project it is used for transforming three-phase voltages and currents to two-phase. This two-phase representation is called alpha-beta frame or stationary frame. The following equations explain the Clarke transformation for three-phase currents but can also be used for voltages [2]

$$i_\alpha = \frac{2}{3}i_a - \frac{1}{3}(i_b + i_c) \tag{2.1}$$

$$i_\beta = \frac{2}{\sqrt{3}}(i_b - i_c) \tag{2.2}$$

or,

$$\begin{bmatrix} i_\alpha \\ i_\beta \end{bmatrix} = \begin{bmatrix} \frac{2}{3} & -\frac{1}{3} & -\frac{1}{3} \\ 0 & \frac{1}{\sqrt{3}} & -\frac{1}{\sqrt{3}} \end{bmatrix} \times \begin{bmatrix} i_a \\ i_b \\ i_c \end{bmatrix} \tag{2.3}$$

This can also be done the opposite direction, from two-phase stationary frame to three-phase signals, using the Inverse Clarke transformation

$$i_a = i_\alpha \tag{2.4}$$

$$i_b = \frac{-i_\alpha + \sqrt{3}i_\beta}{2} \tag{2.5}$$

$$i_c = \frac{-i_\alpha - \sqrt{3}i_\beta}{2} \tag{2.6}$$

or,

$$\begin{bmatrix} i_a \\ i_b \\ i_c \end{bmatrix} = \begin{bmatrix} 1 & 0 \\ -\frac{1}{2} & \frac{\sqrt{3}}{2} \\ -\frac{1}{2} & -\frac{\sqrt{3}}{2} \end{bmatrix} \times \begin{bmatrix} i_\alpha \\ i_\beta \end{bmatrix} \tag{2.7}$$

2.2.3 Park

It can sometimes be beneficial to use real-valued vectors instead of complex space vectors. This can be done by transforming two-phase currents or voltages into a rotating reference frame, also called direct- and quadrature frame (dq-frame), using the Park transformation [2]

$$i_d = i_\alpha cos(\theta) + i_\beta sin(\theta) \tag{2.8}$$
$$i_q = i_\beta cos(\theta) - i_\alpha sin(\theta) \tag{2.9}$$

or,

$$\begin{bmatrix} i_d \\ i_q \end{bmatrix} = \begin{bmatrix} cos(\theta) & sin(\theta) \\ -sin(\theta) & cos(\theta) \end{bmatrix} \begin{bmatrix} i_\alpha \\ i_\beta \end{bmatrix} \tag{2.10}$$

Similarly, the reverse transformation, from rotating reference frame to stationary, can be done using the Inverse Park transformation

$$i_\alpha = i_d cos(\theta) - i_q sin(\theta) \tag{2.11}$$
$$i_\beta = i_q cos(\theta) + i_d sin(\theta) \tag{2.12}$$

or,

$$\begin{bmatrix} i_\alpha \\ i_\beta \end{bmatrix} = \begin{bmatrix} cos(\theta) & -sin(\theta) \\ sin(\theta) & cos(\theta) \end{bmatrix} \begin{bmatrix} i_d \\ i_q \end{bmatrix} \tag{2.13}$$

2.3 Control of an induction machine

To control the operation of an IM the voltage supplied to the stator needs to be regulated and controlled in a manner that satisfies the implemented control. There are many different methods for controlling an IM, with some being very simple and some quite complex. Here two control methods will be explained.

Volts by Hertz (V/Hz) is a simple control program that proportionally changes supplied voltage amplitude depending on the requested frequency. In this way the speed can be controlled, but the torque cannot. This control is typically open-loop, i.e there is no feedback in the system.

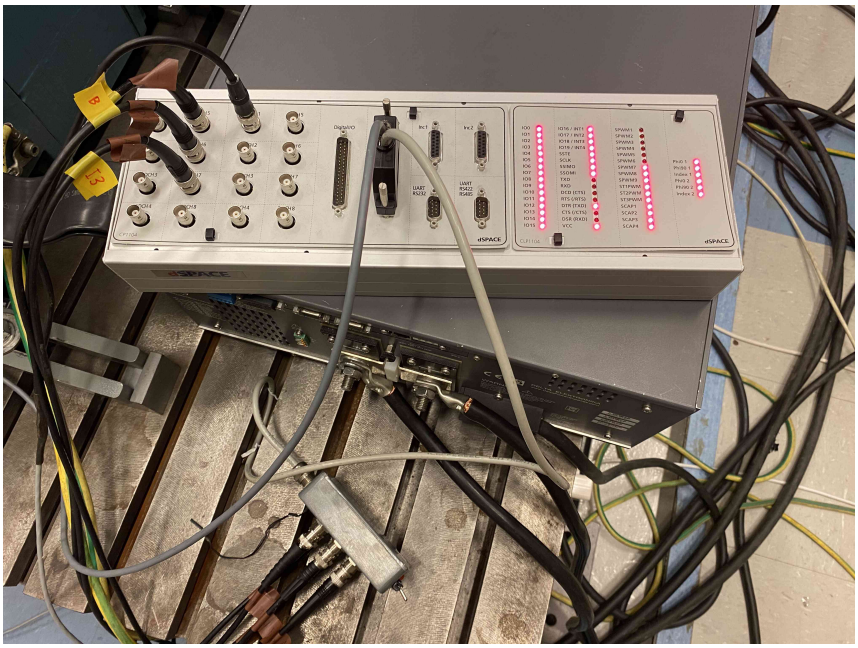

Figure 2.3: The dSPACE DS1104 controller board with connections.

Field-oriented control (FOC) is a more complex method that relies on individually controlling the d- and q-currents to steer the machines operation. This control is typically closed-loop, i.e some variable outputs are fed back as inputs to the program.

In the analysis part of the report these control methods will be explained in more detail.

2.4 Programs

2.4.1 dSPACE

dSPACE DS1104 is a R&D controller board. Together with the program dSPACE controldesk it is used to send and receive signals, ultimately realising real-time operation. In this project it is used as a platform for the control programs created in Simulink to be able to use them for real control and measurements. A picture of the board used for this project is shown in figure 2.3.

2.4.2 Simulink

Simulink is an extension of MATLAB with a block diagram environment. It is used for designing the control programs and also for simulating operation of an IM with the control programs.

3
Case set-up

3.1 Main task

The main task and goal of this project was to be able to control and evaluate the IM. To control the machine and be able to run it in different operational points a control program is needed. The control program was created in Simulink. dSPACE was used to link the program in real-time to the physical IM. Using an inverter, an IM, a control system and some measurement tools the machine was operated in some specific operation modes. During this performance test measurements were taken in order to evaluate the machine's torque ripple and losses. The performance test was also simulated in Simulink and the results were compared with the real measured results.

3.2 Work procedure

The work began with a study of the theory behind the control systems that were created in this project. With the acquired knowledge a goal was set to successfully control the d and q currents with the FOC in Simulink. Simultaneously the V/Hz control was developed and tested through simulations in Simulink.

With the controllers mostly finished and ready for real life testing the focus was switched to the parameterization of a smaller machine. The thought was to use a small 2-pole induction machine of 370 W to carry out primary testing and evaluation of the newly created control programs. The parameters were acquired and the controls were tested which led to the discovery of some flaws and inconsistencies within the control programs. The controls were changed and developed accordingly until they were safe and stable enough to be used on a larger machine.

With updated control programs the goal was to successfully control the speed of a large induction machine. This machine, which throughout the report will be called "large machine", was already parameterized and therefore most of the parameters were given. The V/Hz and FOC programs were implemented in dSPACE and eventually successfully used to control the machines operation. The large machine was then loaded with a DC-machine during a performance test and the results were recorded. The performance test was also simulated in Simulink, which had the goal of being as identical to the real test as possible. With the recorded measurements of stator voltages, currents, speed, torque and estimated rotor flux the performance

as well as losses of the motor were discussed. The differences between measured and simulated results were also discussed.

3.3 Control system

For this project two control systems for an induction machine were created. V/Hz control, which is one of the most simple control methods, was primarily used in the beginning of testing the machine. For the "main" test with the large machine FOC was used.

3.3.1 V/Hz

The V/Hz control was done as an open-loop control. The control has speed reference as an input. Depending on the speed reference the control will decide the frequency and the amplitude of the stator voltages. In turn the switch signals sent to the inverter will be generated.

3.3.2 FOC

The FOC was done as a closed-loop control. The FOC's main objective is to control the stator voltages to achieve the requested speed of the motor. This should be done in a manner that satisfies the requested d and q currents. The program will have two PI-regulators of the first order. One for the torque reference and one for the voltage reference. With the input of speed reference the control should calculate the torque reference for the motor. The torque reference is then used for generating the appropriate d and q current references. The d and q current references is then used for generating the corresponding d and q voltage references, which through transformations is transformed to three-phase voltage references. The voltage references is then used to generate the correct signals to be sent to the inverter switches and thus the inverter will generate the requested voltage supply. As this control is closed-loop the speed and currents should be fed back and used in the control.

3.4 Tests and measurements

The small machine that was used as a testing and development platform for the controllers was present in two parts of the project, with the first one being parameterization of the small machine. During this part a no load test, locked rotor test and a "DC-test" resistance measurement were conducted. These tests were done in a lab environment with access to a coupling desk and preconfigured measurement connections for measuring voltage, current and power. As a result the parameters of the machine could be estimated and then used in the control programs and for simulations.

The other testing and measurement part, during which the small machine was used, was for testing of the V/Hz and FOC controls. These tests were conducted in another lab environment where more connections had to be done manually. The inverter, dSPACE I/O connection board, the small machine and measurement tools had to be connected.

The large machine was first operated with V/Hz control in order the check the condition of the machine and verify the connections. FOC was then used for the test which was recorded and analysed. Measurements of voltages, currents and torque were made through a device called picoscope, whilst speed and estimated rotor flux were measured through dSPACE control desk. The test included a magnetisation period, a speed reference step and a load torque step and was conducted over a 20 second period. An identical test was implemented and simulated in Simulink.

4
Analysis Part

Here the work and the obstacles encountered throughout the project is presented. The results from the tests, explanations of the control programs and how the measurements were taken is displayed in this chapter.

4.1 Volts/Hertz

V/Hz control is a traditional and simple open-loop control technique used for speed control of inverter-fed induction machines. The main method of V/Hz is to vary the stator frequency to linearly decide the voltage fed to the IM. The linear relation between frequency and voltage means that when the frequency is zero the voltage will be zero, and when the frequency reaches base value (max value) the voltage also reaches max value. The relation between frequency and voltage comes from the desire to keep the flux constant. It is based on the steady-state stator voltage equation [4]

$$U_s = R_s I_s + j\omega_1 \psi_s \tag{4.1}$$

If the voltage drop over the stator resistance $R_s I_s$ is neglected in (4.1) we get the following relation

$$\frac{U_s}{w_1} \approx \psi_s = C_{V/Hz} \tag{4.2}$$

which will be called the V/Hz constant $C_{V/Hz}$ throughout the report. In figure 4.1 a normal V/Hz operation is displayed.

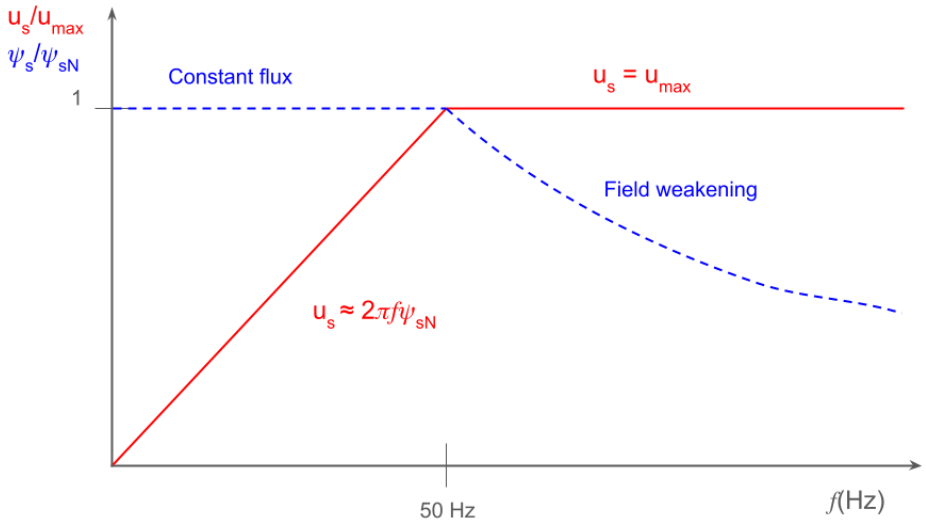

Figure 4.1: A graph showing a typical V/Hz control where f, u_s, u_{max}, ψ_s and ψ_{sN} are the frequency, stator voltage amplitude, maximum voltage of the inverter, stator flux amplitude and nominal stator flux, respectively. It can be seen that the voltage u_s and the frequency f are proportional until base speed is reached (50 Hz). After that the field weakening begins.

By keeping the flux constant the V/Hz control can provide constant torque up to base speed. When base speed is reached the maximum voltage is also reached. The maximum voltage cannot be exceeded but the frequency can still be increased at the expense of losing some torque capability. This is called field weakening.

For the project this has been implemented in Simulink. With the use of the relation in (4.2) the desired synchronous speed ω_{1ref} (input) is multiplied with the stator flux reference ψ_{sref} (constant) to calculate the reference stator voltage amplitude u_{sref}

$$u_{sref} = \psi_{sref}\omega_{1ref} \tag{4.3}$$

The voltage reference is then put in to the stationary frame by giving it a rotation

$$U^s_{sref} = u_{sref}e^{j\theta_1} \tag{4.4}$$

$$U^s_{sref} = u_{s\alpha} + ju_{s\beta} \tag{4.5}$$

where U^s_{sref} is the complex representation of the voltage reference in the stationary frame. $u_{s\alpha}$ and $u_{s\beta}$ are the voltages in alpha and beta direction. θ_1 is the rotational angle which is the integral of the speed reference ω_{1ref}.

After the voltage reference in alpha and beta directions has been made it is transformed to three-phase voltages u_{sa}, u_{sb} and u_{sc} using the inverse-clarke transform. It is with these reference phase voltages that the pulse width modulation (PWM) control signals are created and sent to the inverter, which in turn generates the actual three-phase voltages fed to the IM. In Simulink the built-in induction machine

model has been used. The output current of the IM block is in three-phase so this is transformed to alpha-beta using the clarke transform.

The full Simulink model for V/Hz used in this project can be found in appendix A.1.

4.2 FOC

The FOC is a closed-loop control. The FOC consists of a number of blocks, each block in the system has some inputs and provides the requested outputs. The FOC's main objective is to control the stator voltages to achieve the requested speed of the motor. This should be done in a manner that satisfies the requested d and q currents. The full Simulink model for the FOC used in this project can be found in appendix A.2.

4.2.1 Current Regulator

By using a current regulator the idea is to be able to control the torque more precisely. This is because the torque is a direct result of the armature current. The starting currents are also kept lower with a current regulator, as the currents are directly controlled and this causes less tearing of the motor. [2]

The current regulator uses a PI-regulator and the gain constants are selected based on the parameters of the machine and the required rise time of the process. The idea of the current regulator is that the closed loop system should be a first order low pass filter [5] and so the closed loop system with the PI constants can be formulated as

$$F_c(s) = k_{pc} + \frac{k_{ic}}{s} = a_c\hat{L_\sigma} + \frac{a_c(\hat{R_R} + \hat{R_S})}{s} \tag{4.6}$$

and that the proportional k_{pc} and integration k_{ic} constants are based on the parameters of the machine and a_c which is dependent on the required rise time

$$a_c = \frac{log(9)}{Rise\ Time\ [s]} \tag{4.7}$$

$$k_{pc} = a_c\hat{L_\sigma} \tag{4.8}$$

$$k_{ic} = a_c(\hat{R_R} + \hat{R_S}) \tag{4.9}$$

Later in the project an anti-windup part was added to the current regulator. This was done by adding a feedback of the control signal to the input of the I-regulator.

4.2.2 Flux Observer

In order to estimate the flux in the rotor the current model (CM) was used. The CM needs a speed sensor to measure the rotor speed of the machine. One very good property of the CM is that it is the only known flux estimator that is particularly

stable for low speed operations [2]. This is extra sought after in this project since one of the main obstacles might be to get the machine to rotate at all.

The method used in this project is the indirect field orientation (IFO) rather than the direct field orientation (DFO) based on the preference to work with constant quantities in the steady state and that w_1 is an explicit variable in the control system for IFO [2].

The created controller for flux estimation is based on these relations for the induction machine

$$\hat{\psi_R} = i_{sd}\frac{\hat{R_R}}{s + \frac{\hat{R_R}}{\hat{L_M}}} \tag{4.10}$$

$$\hat{w_2} = \frac{\hat{R_R}\hat{i_{sq}}}{\hat{\psi_R}} \tag{4.11}$$

$$\hat{w_1} = w_r + \hat{w_2} \tag{4.12}$$

$$\hat{\theta_{rf}} = \hat{\theta_1} = \int \hat{w_1} dt \tag{4.13}$$

4.2.3 Speed Regulator

The idea of the speed regulator is to be able to keep the speed constant over time regardless of external disturbances. The speed regulator works similar to the current regulator as it utilises a PI-regulator to regulate the error between the requested and measured speed. The speed regulator compares the requested speed with the measured speed of the motor and the resulting error is multiplied with a proportional constant and integrated and multiplied with an integrating constant. The proportional and integrating constants are based on the characteristics of the machine and are based on the following relations [6]

$$a_w = \frac{log(9)}{Rise\ Time\ [s]} \tag{4.14}$$

$$k_{pw} = a_w \hat{J} \tag{4.15}$$

$$k_{iw} = a_w \hat{B} \tag{4.16}$$

The resulting output from the speed regulator is the requested torque that the machine needs to adjust to the correct speed.

An anti windup was also implemented in the speed regulator since if the requested torque could not be realised because the requested currents became too high, then the integrator would keep increasing the requested torque so that it became unreasonably high. It would thus take a while for the PI-regulator to wind-down until it could request reasonable torques again. With the anti windup this problem was avoided.

4.2.4 Current Reference Calculator

The idea of the current reference calculator is to calculate the correct currents based on the requested torque and flux and the parameters of the machine. The calculator also takes into account the rated current of the machine and limits the currents accordingly. If the requested torque is limited, it will be sent back to the anti windup in the speed regulator.

A field weakening calculation is also implemented in this block. If the speed of the motor is above the speed for field weakening the flux will be decreased proportionally to the speed of the motor.

4.3 PWM signals

A three phase inverter is able to produce six voltage vectors and two zero vectors but to be able to use any voltage vector inside the hexagon, PWM has to be used. For linear modulation the maximum magnitude of the voltage vector is the circle inside the hexagon in figure 4.2 and the radius of the circle is $u_{max} = U_{dc}/\sqrt{3}$ [7].

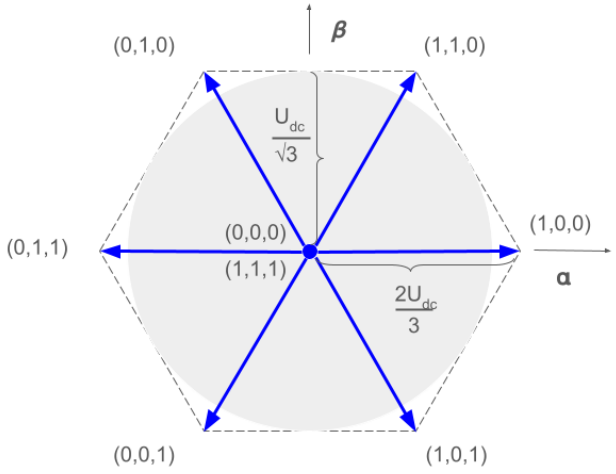

Figure 4.2: The switching states of a three phase inverter, six voltage vectors and two zero vectors. With PWM and linear modulation all voltage vectors inside the circle can be accessed.

To create PWM signals the idea is to compare the control signals with a triangular carrier wave to generate the correct switching pattern for the three phase inverter. To do this the control signals have to be normalised to go between 0 and 1 just like the carrier signal. By dividing the original sinusoidal voltage waveforms with U_{DC} the new signal will move between $\frac{1}{2}$ and $\frac{-1}{2}$ and by adding $\frac{1}{2}$ the new signal will go

between 0 and 1 according to

$$d_a = \frac{1}{2} + \frac{u_{a,ref}}{U_{DC}} \tag{4.17}$$

$$d_b = \frac{1}{2} + \frac{u_{b,ref}}{U_{DC}} \tag{4.18}$$

$$d_c = \frac{1}{2} + \frac{u_{c,ref}}{U_{DC}} \tag{4.19}$$

This new control signal with a duty cycle from 0 to 1 will then be compared to the carrier wave. However the problem with this technique is that only 87% of the radius of the circle inside the hexagon can be used.

To solve this problem and to extend all the way out in the circle a new sine wave is added to the signal with a frequency three times the fundamental frequency [7]. This new sine wave is called the zero sequence,

$$\Delta = -\frac{min(u_{a,ref}, u_{b,ref}, u_{c,ref}) + max(u_{a,ref}, u_{b,ref}, u_{c,ref})}{2} \tag{4.20}$$

$$\tag{4.21}$$

and by adding the zero sequence to the other signals the new duty ratios for the signals is created

$$d_a = \frac{1}{2} + \frac{u_{a,ref+\Delta}}{U_{DC}} \tag{4.22}$$

$$d_b = \frac{1}{2} + \frac{u_{b,ref+\Delta}}{U_{DC}} \tag{4.23}$$

$$d_c = \frac{1}{2} + \frac{u_{c,ref+\Delta}}{U_{DC}} \tag{4.24}$$

and with these new duty ratios the whole circle in 4.2 can now be accessed.

4.4 Inverter

It is the inverter that uses the generated duty ratios to generate the real voltage signals. In real applications this is done by comparing the duty ratio signals to a triangular carrier wave, which in turn decides when the switches of the inverter should turn on or off. The particular sequences of switching as a result of the duty ratios sent to the inverter will generate a PWM sine voltage wave. In the simulations a built-in inverter block was used. For the real measurements a real inverter is used.

4.5 Small Induction Machine

Since the large machine had low resistances there was some concern that the starting currents might get too high. Too avoid this it was decided that the controls would be tested on a smaller machine first in order to minimise the risk of damaging the large machine in any way. Before the tests on the small machine could be performed the parameters had to be measured. The machine nameplate is shown in figure 4.3.

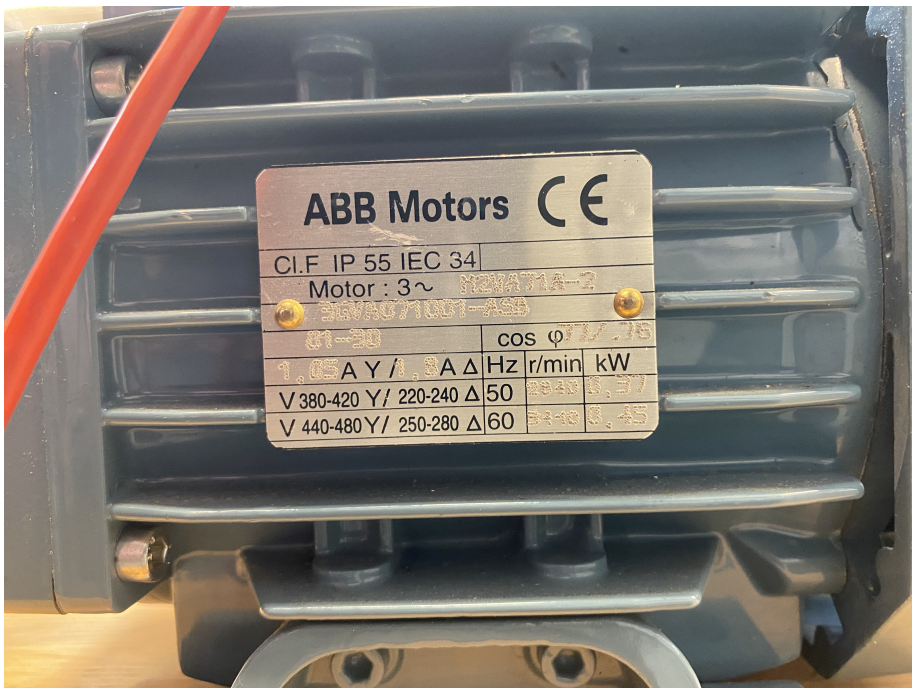

Figure 4.3: The nameplate of the small induction machine used for testing the controllers. It has a rated power of 0.37 kW and nominal speed of 2840 rpm when operated with a 50 Hz voltage source.

4.5.1 DC-test

The DC-test was performed by first applying a DC voltage to the machine and increasing it until rated current was reached. Thereafter a multimeter was used to measure the voltage drop over two of the stator windings, since the machine was star-coupled. The resistance of the stator windings R_s was calculated by using the following formulas

$$R_{DC} = \frac{U_{DC}}{I_{DC}} \tag{4.25}$$

$$R_s = \frac{R_{DC}}{2} \tag{4.26}$$

4.5.2 Locked Rotor test

The locked rotor test was done using a lower source voltage than the grid due to the fact that it was preferable to keep the shaft torque reasonably low. Even though this makes the parameters a little more inaccurate it was necessary to prevent or at least minimize the risk of damaging any equipment, as the chosen method of locking the rotor was not the most reliable choice.

First the grid supply was connected to a star-delta connected three-phase transformer of 230/130 V giving a line-to-line voltage of 130 V. After the transformer a variable autotransformator was connected allowing the source to be varied through turning a knob. Then the motor was connected. The rotor of the IM was locked by wrenching the motor in place and attaching a metal bar to the rotor keeping it in place when the rotor starts rotating against the table. This can be seen in figure 4.4.

The parameters approximated from the locked rotor test were rotor resistance R_r, stator leakage inductance $L_{s\sigma}$ and rotor leakage inductance $L_{r\sigma}$. During the test the voltage was gradually incremented up to about 26 V where the voltages, currents and powers were recorded. The parameters were then calculated using the following relations

$$R'_r = \frac{P_{3ph,lockedrotor}}{3I^2_{s,lockedrotor}} - R_s \tag{4.27}$$

$$X_s + X'_r = \frac{Q_{3ph,lockedrotor}}{3I^2_{s,lockedrotor}} \tag{4.28}$$

$$X_s = X'_r = \frac{X_s + X'_r}{2} \tag{4.29}$$

$$L_{s\sigma} = L'_{r\sigma} = \frac{X_s}{2\pi f} \tag{4.30}$$

4.5.3 No Load test

For the no load test the IM was direct started through a direct connection to the grid (400 V and 50 Hz) and operated at a speed close to base speed (3000 rpm) with no torque load. This was done to get a good approximation of the parameter values. The parameter that could be approximated from the no load test was the magnetizing inductance L_m. The voltage, current, active power and reactive power was measured during operation. Magnetizing inductance L_m was then calculated according to

$$X_m = \frac{Q_{3ph,noload}}{3I^2_{s,noload}} - X_s \tag{4.31}$$

$$L_m = \frac{X_m}{2\pi f} \tag{4.32}$$

4.5.4 Parameters

The estimated parameters of the 2-pole 370 W IM extracted from the tests are shown in table 4.1.

Table 4.1: The estimated parameter values of the 370 W induction machine in T-model representation

Parameter	Value	Unit
R_s	15.19	Ω
R_r	14.79	Ω
$L_{s\sigma}$	0.04	H
$L_{r\sigma}$	0.04	H
L_m	0.99	H

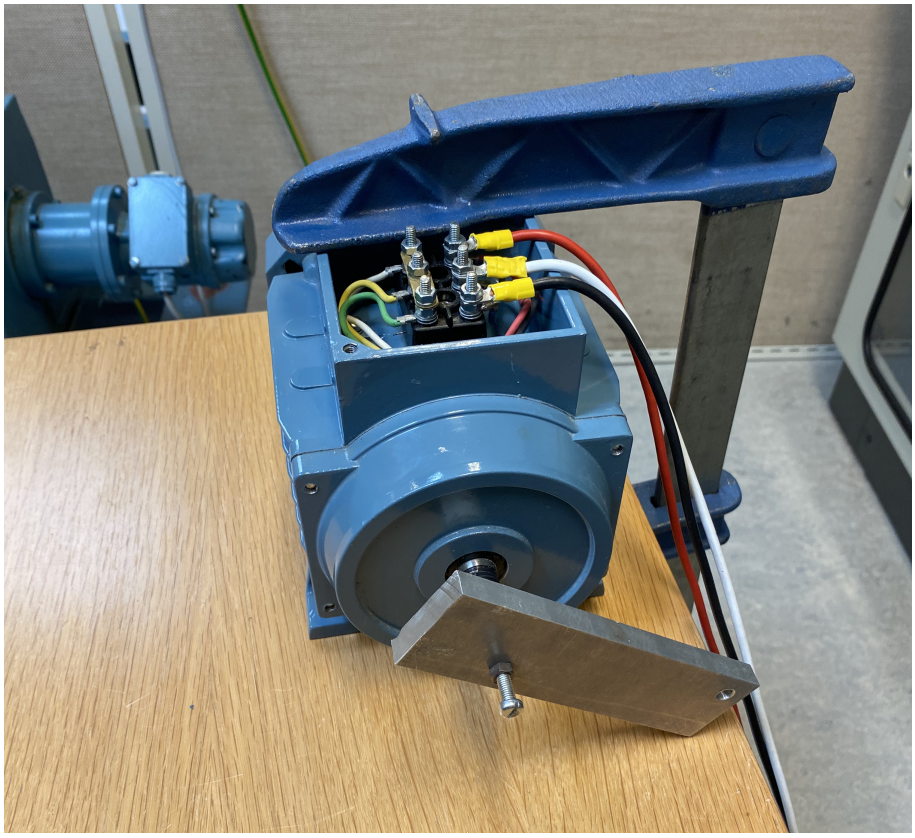

Figure 4.4: The 370 W induction machine wrenched stuck to the table with a locked rotor.

Figure 4.5: The incremental encoder giving 5000 pulses per revolution used for operating the small machine.

4.5.5 Measurements for parameter tests

For the parameter tests the currents and voltages were measured and transferred to an existing computer program that could calculate the active and reactive power. These tools were already available in the laboratory.

4.5.6 Measurements for the dSPACE controller

To be able to control the machine in real time with FOC, measurements of speed and current had to be provided to the dSPACE control board.

4.5.6.1 Speed Measurement

Speed was measured using an encoder mounted on the rotor shaft, shown in figure 4.5. The incremental encoder that was used [8] is sending 5000 pulses per revolution and uses two pulse trains, A and B, which makes it possible to detect the direction of rotation. By counting the pulses, the position and speed of the motor is measured. The small machine did not have an encoder attached, so this encoder was brought from another machine and retrofitted onto the shaft of the small machine.

The dSPACE built in encoder-reader block did an average of the 4 latest samples every time it sent a pulse. This made it so that the rpm measurements only could be read at a 30 rpm accuracy (30, 60, 90, 120...). Therefore a secondary delay and average was implemented over 30 samples to get a better rpm resolution (1 rpm accuracy). However, it was suspected that this introduced a delay in response time

which would affect the overall stability of the program. That is why it was decided to settle for a little lower resolution of 5 rpm accuracy.

4.5.6.2 Current Measurement

Zero flux ampere sensors in the inverter were used for current measurement. The current carrying cables were wound 5 times through the current sensors to amplify the signal 5 times. Some calibration was done with the help of a normal multimeter. The multimeter was connected between the inverter and machine to measure the current and then compared with current seen in dSPACE to identify the differences. There was a little difference, but a gain of 100 was chosen. Throughout testing the control programs some disturbances in the measured current were identified when PWM was active.

4.5.6.3 Other measurements

Voltages and torque were not measured for the small machine. The estimated rotor flux calculated in the flux observer was measured in dSPACE.

4.5.7 Testing the controllers

At this point the controllers was tested in reality. The problems and results of the tests are summarised here.

4.5.7.1 V/Hz

The Simulink model had to be altered to fit the dSPACE environment and to link the outputs and inputs of the dSPACE DS1104. The Simulink file was built (compiled) and the sdf file that was generated from building the model was transferred into the dSPACE controldesk program. From there the speed input could be varied and the measurement of stator currents could be viewed. For the PWM to work a dSPACE block for 3-phase PWM generation was used to generate the six switch signals by using the duty cycle signals and comparing it to a carrier wave. The PWM frequency was set to 10 kHz. An attempt at using a 50 microsecond deadband was made, but then the motor could only reach about 200 rpm. The DC-supply was only 70 V, and could in practice only reach 60 V, which is why the flux in the machine became lower. Therefore we kept the rated V/Hz constant $C_{V/Hz}$

$$C_{V/Hz} = \frac{400\sqrt{\frac{2}{3}}}{50 \cdot 2\pi} \tag{4.33}$$

to keep the V/Hz relation constant to when the new (60 V) voltage maximum was reached. This meant that flux weakening started earlier.

4.5.7.2 FOC

The maximum voltage saturation of the current regulator was previously set to saturate the d and q amplitudes individually, which was in fact wrong. Instead this was changed so that the combined complex amplitude of d and q voltages was saturated. During the first testing of the FOC the program was sometimes unstable. The first around 20 seconds of turning on the PWM signals gave a very high q current (ca 1.6 A) and after these 20 seconds the amplitude fixed itself and jumped down to its expected value of around 0.7 A. This was fixed with the implementation of an anti-windup mechanism in the current regulator, which compensated for the very high values that the PI-regulator was generating at the beginning of running the program (because of the high "error").

It was realised that the flux of 0.65 Wb was probably very high. When the saturation and anti-windup had been implemented it was found that when the reference currents were used for the flux observer high speeds could be reached for the machine. However when using the measured currents as input to the flux observer only a speed of around 300 rpm was reached. We remembered that when running the previous versions of the FOC the flux was hovering at around 0.2 or 0.3 Wb when the flux ref was around 0.7 Wb. When using a new flux reference of 0.13 and using the anti-windup the speed could go up to around 1800 rpm again.

Direct starts have been tested for both the V/Hz controller and the FOC and the maximum current that was reached was about 1 A, which is okay since the rated current is 1.05 A. The FOC has a maximum current set at rated but the V/Hz does not. However a maximum voltage is implemented and a reality in both controllers since the DC-supply is only 60 V. So this will reduce the possibility of extremely high currents since the stator resistance Rs is 15 Ω.

4.6 Large Machine

The large machine is an induction machine however the parameters and much of the information about the machine was unknown.

4.6.1 Parameters

The parameters for the large machine were provided by a PhD student that had conducted the parameter tests on the machine. The parameters for the large machine was given according to Table 4.2

Table 4.2: The estimated parameter values of the large induction machine in T-model representation

Parameter	Value	Unit
R_s	17.78	$m\Omega$
R_r	9.5	$m\Omega$
$L_{s\sigma}$	0.0495	mH
$L_{r\sigma}$	0.0495	mH
L_m	1.7005	mH
p	2	

.

The parameters inertia J and mechanical damping B was not estimated. They were assumed to be: $J = 0.01$ and $B = 0.01$. This probably impacted the accuracy of the speed regulator since these parameters are used for deciding the gains of the PI-regulator in the speed regulator. This will also lead to some differences between the Simulink IM model and the real IM which will lead to differences in the simulated and measured data.

4.6.2 Measurements

In order to be able to control the machine in real time and to analyse the results of the tests, it was necessary to carry out appropriate measurements. The measurement of speed and current was essential to control the machine in real time with FOC. Voltages and torque were measured to be able to analyse the results after the test.

Measurements taken from dSPACE were measured with a sample frequency of 10kHz while measurements with the picoscope were done using 200kHz sample frequency.

4.6.2.1 Speed Measurements

To measure the speed a DRBK torque sensor [9] was used, which had a built in encoder. The encoder used to measure the speed of the large machine only had one pulse train available, which was pulse train A. This meant that the encoder could

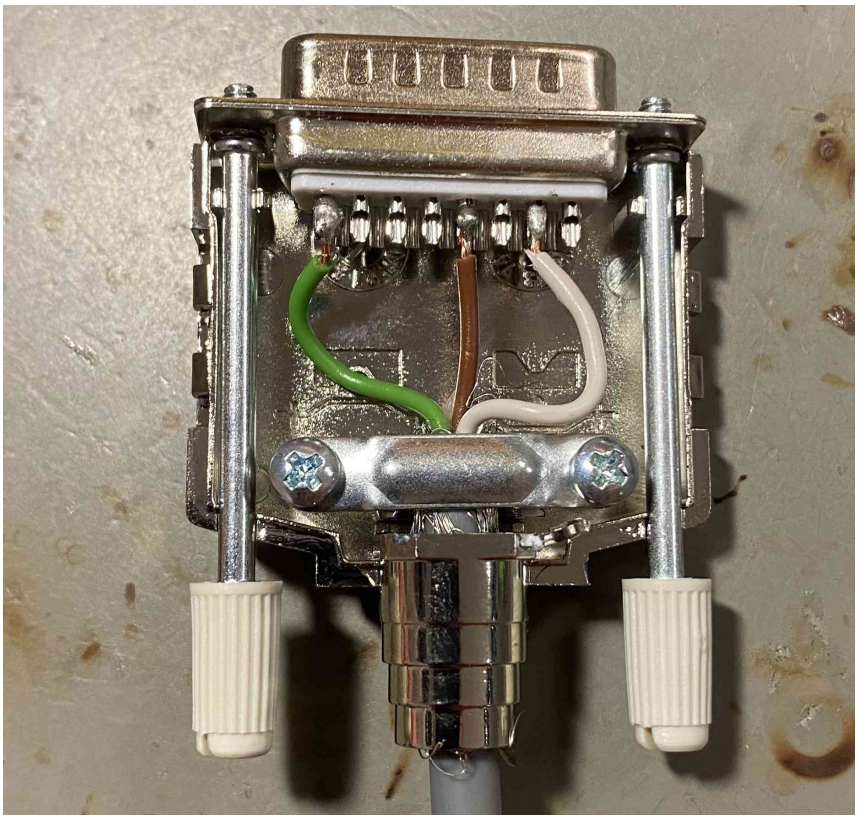

Figure 4.6: Wires from the encoder soldered onto a digital I/O connector. This picture was taken during the first attempt of measuring the speed in dSPACE. However when the frequency block in dSPACE was implemented, the white and green cables which contains pulse train A and ground was soldered to another digital I/O connector with 37 pins to be processed in dSPACE.

not identify which direction the shaft was spinning. To get the pulse train A to be measured in dSPACE the wire that sends the signal had to be connected to the dSPACE board. While another wire from the DRBK torque sensor was connected to the picoscope to measure the torque. The correct wire that sent the signal for pulse train A was identified in the cable and it was connected to the dSPACE board by soldering it to the Slave I/O PWM cable. It was soldered there because that is where the dSPACE block could count the frequency of the pulses.

The encoder could only send 60 pulses/revolution compared to the 5000 pulses/revolution that the encoder for the small machine could send. So when the same technique was used as for the small machine a long delay was introduced since we would have to wait for longer now before a pulse was sent to the controller. Using the same technique as for the small machine and requiring a precision of 5 rpm for the speed measurement resulted in a delay of 0.1 s. This delay caused the control system to become unstable.

The delay of the speed measurement was 0.1 s so the rise time of the speed con-

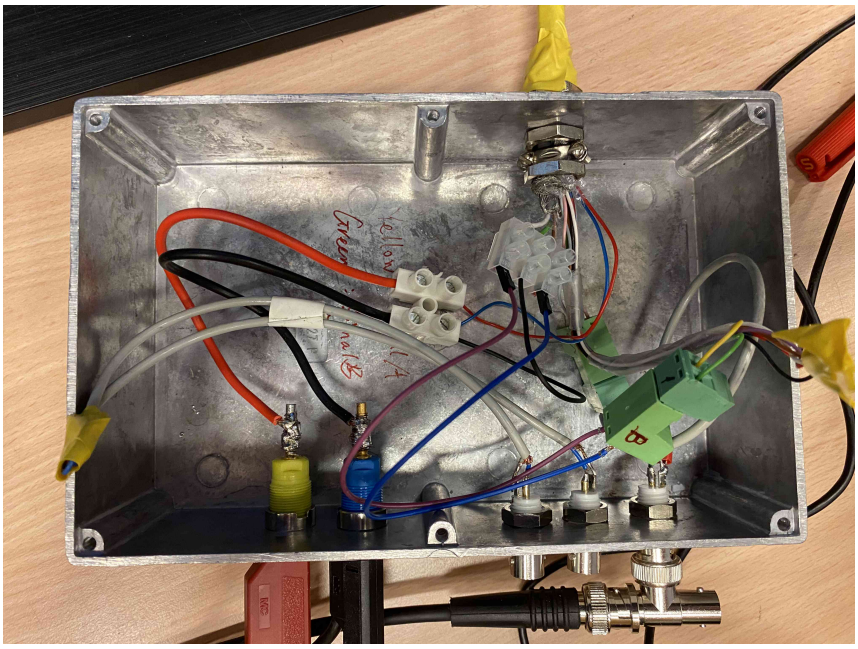

Figure 4.7: The wires from the cable of the DRBK torque sensor was connected to different inputs. The wire that measured torque was connected to the picoscope. The wire that measured the speed was connected to dSPACE. Power is provided here to the DRBK torque sensor.

troller was set to be larger than the delay so that the system would not become unstable. The rise-time was set to 0.4 seconds. However now there would be large current ripples each 0.1s when the speed was updated. This phenomena had not been discovered in the simulations probably due to the very low inertia and mechanical damping of the real machine. Since when inertia and mechanical damping was severely decreased in the simulations the process became unstable just like for the real machine. However this was not seen in the original simulations since the inertia and mechanical damping was assumed to be larger than they actually might have been for the real machine. To get rid of the substantial current ripples the rise time of the current regulator was also increased but to 0.04 seconds. 10 times faster than the speed regulator. Now the response of the system is slower than before but it is more stable.

It was discovered that another method could be used to measure the speed without causing a big delay to the control system. The new speed measurement method used a dSPACE block in Simulink that measured the frequency of the pulse train from the encoder. Since B pulses was not used for the DRBK encoder, all speed was interpreted as positive. So even if the shaft was rotating backwards a positive speed would be measured. Since this encoder only sends 60 pulses/revolution the speed measurement was prone to some disturbances. To remove most of the noise, a low-pass filter was added after the speed measurement to get rid of oscillations and make the control system more stable.

4.6.2.2 Picoscope Measurements

The picoscope could be used and viewed on 2 screens next to the computer from where the machine was controlled. The programs made it possible to record and save the measurements for post processing. The picoscope measured voltage, currents and torque. The currents are shown in volts, however 1 mV is equal 1 A, so a gain of 1000 is used. For the voltages 1 mV in the picoscope equals 10 mV in reality so a gain of 10 was used. Temperature in the rotor and stator could also be viewed with another program.

For the torque a gain of approximately 100 is used. The measured torque usually contained lots of oscillations and disurbances. So to be able to read the torque a moving average of the torque had to be implemented when plotting the measurements. The torque measurement also had an offset of -5 Nm, so 5 Nm was added to the results in the post processing.

4.6.2.3 Current Measurements for the Controller

Current was measured from the inverter and the inverter was connected to the dSPACE control board. This was done because the measured currents was used in the controllers and therefore had to be sent to dSPACE.

The zero flux ampere sensors in the inverter cabinet was used for current measurement for the large machine. The current carrying cable only passed through the flux ampere sensor once unlike the current measurements for the small machine which was wound through the flux ampere sensor 5 times. That is why the new gain from the current measurements was 500 instead of 100.

4.6.3 Testing of controllers

At this point the controllers were used to control the large machine. The problems and results of the tests are summarised here.

4.6.3.1 V/Hz

The first test on the large machine was made with the V/Hz control. The objective of the task was to make sure that the controls could control the machine as expected. Before the test was conducted external resistors of around 0.1 Ω was added to the circuit to decrease the possibly high currents. The DC-supply that was used only had 30 V and 200 A as maximum output, but the maximum currents was limited to 95 A. The current was limited to 95 A since the maximum output of the inverter was 100 A.

By using the V/Hz control as described above the machine was successfully rotating. It was noted that during this operation with V/Hz the output currents from

the DC-supply was around 60-70 A when requesting 500 rpm in the control program.

4.6.3.2 FOC

It was noted that the flux was weakened at around 350 rpm. The flux could not reach 0.1 Wb at this speed. This is because the dc supply only supplies a maximum voltage of 30 V. When the speed is increased the impedance of the motor will also increase due to the high inductance and their frequency dependency. This means that when 350 rpm is reached the maximum current of 95 A implemented in Simulink isn't the real maximum output current with the current setup. This leads to that the controller asks for a higher current than the DC supply can deliver.

4.6.4 Experiment

An experiment was conducted to examine the differences between the real large machine and the simulated equivalent of the machine with the estimated parameters.

The experiment was prepared in Simulink to step up certain reference values at specific time intervals. This was done in order to be able to perform an identical simulated experiment. The experiments only had to be manually started and then stopped at an appropriate time.

The test was performed by enabling the PWM switches to turn on and off and therefore starting to magnetise the machine to the requested magnetisation while maintaining a speed of 0 rpm. After 2 seconds the requested speed to the machine was stepped up to 500 rpm. After 8 seconds the DC-machine was stepped up to deliver a load of 9.75 Nm on the IM. The test was completed after 20 seconds. An overview of the connections for the test is shown in figure 4.8.

4.6.4.1 DC-machine

For the experiment a DC-machine was used to act as load on the large machine. The DC-machine was set to be used in torque control. The thyristor inverter of the DC-machine was connected to the dSPACE controller board and the torque could thereby be controlled from the computer. This made it possible to synchronise the load step with the rest of the program.

4.6.4.2 Simulations

The simulated test was performed with the same controllers as for the real test. However instead of the dSPACE input and output connections, the signals was directly connected to a simulated IM with the estimated parameters of the real large machine.

Figure 4.8: A picture showing the connection made between the large machine and the DC machine.

4.6.4.3 Results of the test

The graphs in figure 4.9 to 4.19 shows the measured and the simulated response of quantities from the test conducted on the large machine.

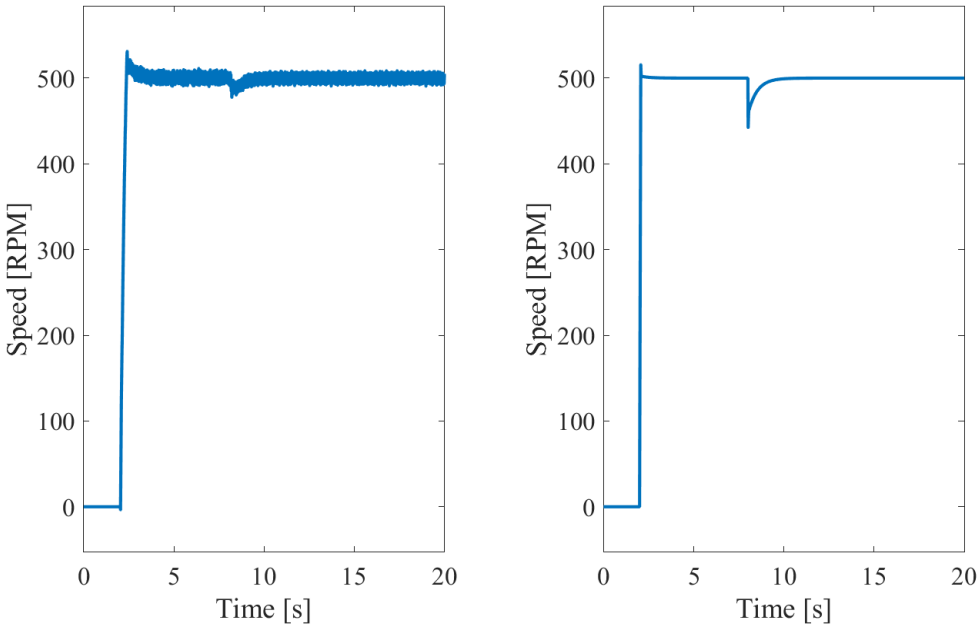

Figure 4.9: The measured (left) compared to the simulated (right) speed test response. In both the graphs some overshoot from the speed reference step can be seen. It is also clearly seen that the speed momentarily drops when the DC-machine begins to put a load torque on the shaft of the large machine.

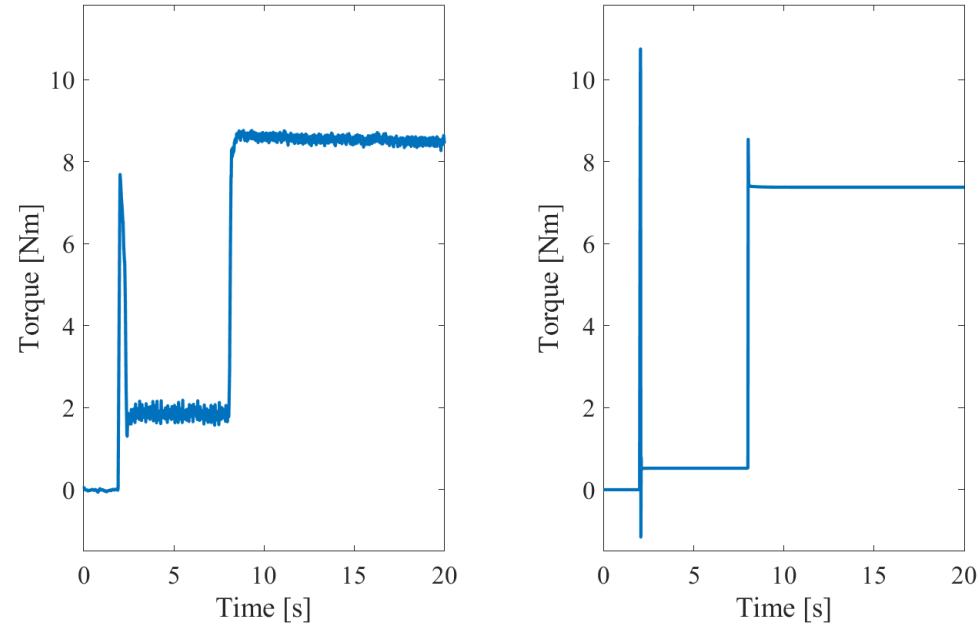

Figure 4.10: The measured (left) compared to the simulated (right) torque test response. It can be seen that when the speed reference is stepped, there is some immediate torque for both the measured and simulated tests. During steady-state operation the simulated torque is stable, however for the real machine the torque experiences minor oscillations.

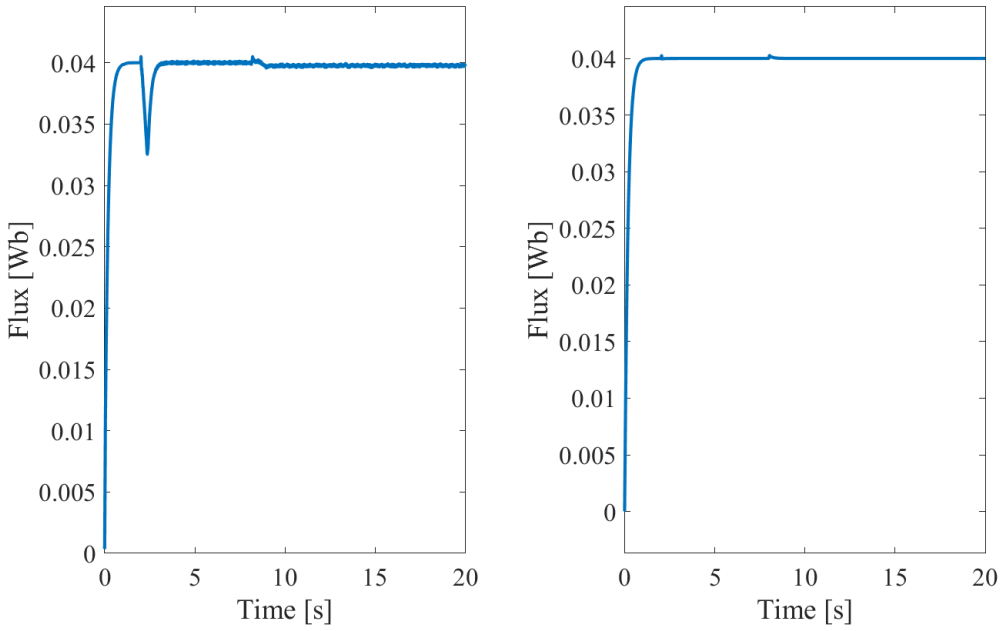

Figure 4.11: The measured (left) compared to the simulated (right) estimated rotor flux test response. Both achieved the required rotor flux quite smoothly. However, when the speed for the machine is turned on, they both seem to get a ripple, the ripple for the real machine was greater than for the simulated. When the load torque was added there was another ripple for both tests. This time the magnitude of the ripples were quite similar.

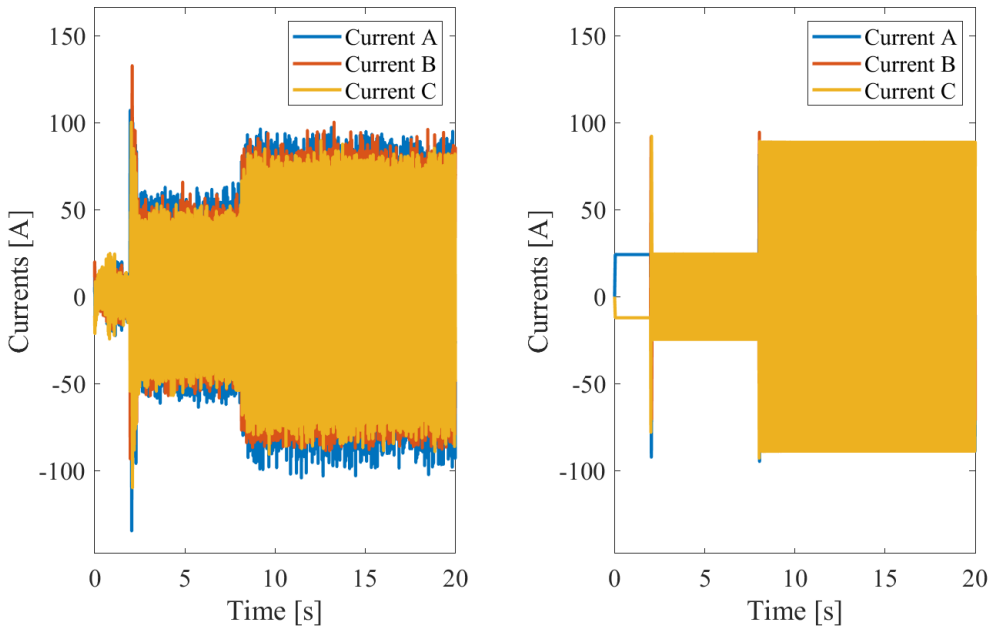

Figure 4.12: The measured (left) compared to the simulated (right) current test response. At 2 seconds, large starting currents can be seen for both tests. At no load the measured currents seem to be larger and at load the tests appear similar in amplitude.

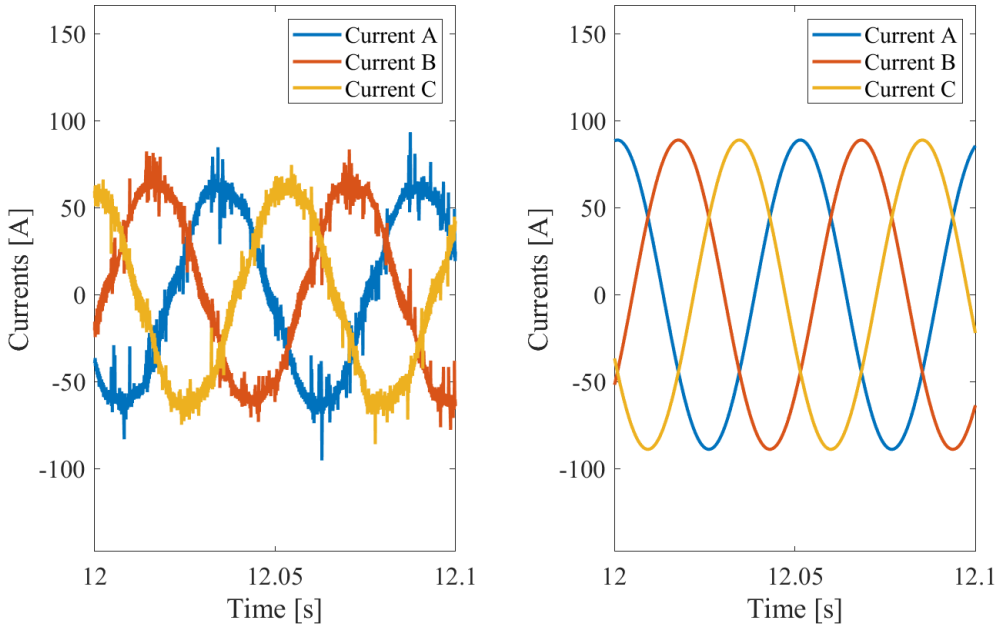

Figure 4.13: The measured (left) compared to the simulated (right) current test response zoomed in between 12 and 12.1 seconds of the test. The amplitude of the simulated current is greater than the measured current. However, there are some large ripples in the measured currents.

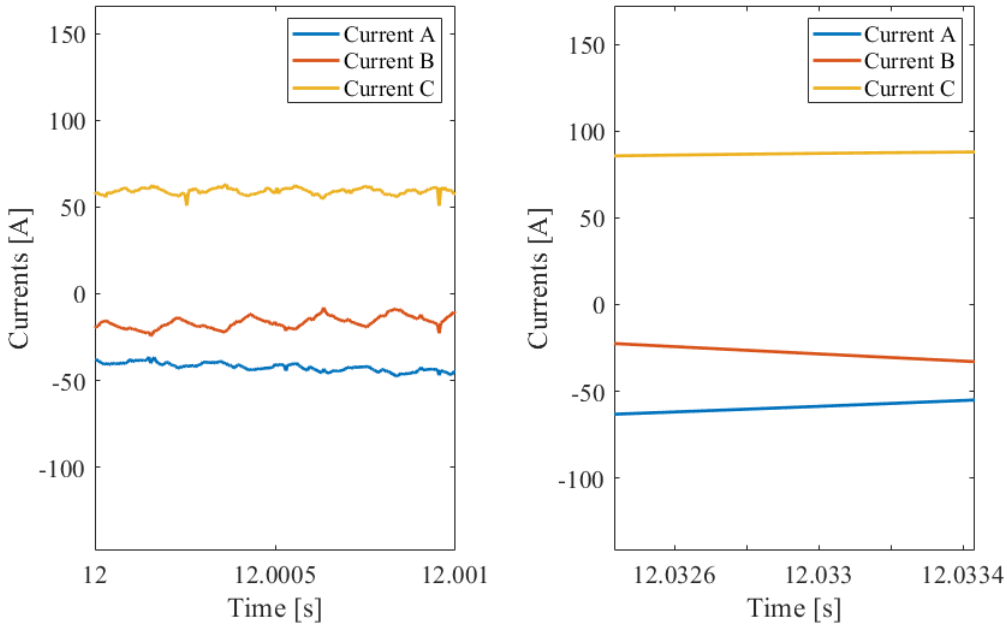

Figure 4.14: The measured (left) compared to the simulated (right) current test response zoomed in at 1 ms intervals of the test. The difference in timings is because of small phase differences between the real and simulated results. The time intervals picked in this figure were chosen in order to make the measurements comparable (for visual purposes).

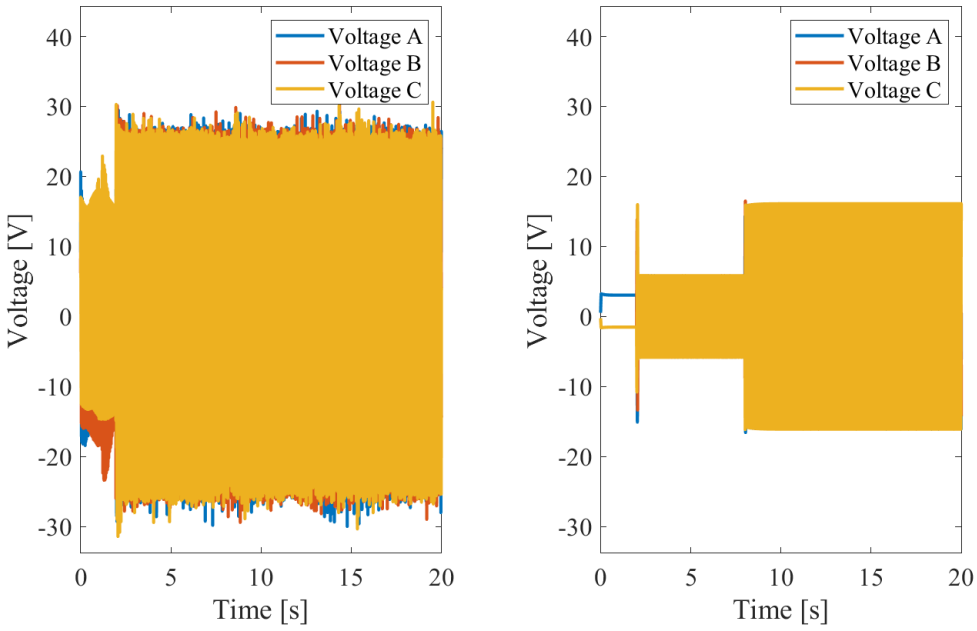

Figure 4.15: The measured (left) compared to the simulated (right) voltage test response. The amplitude of the measured voltages seems to be greater than the simulated voltages. The measured voltage is fairly constant throughout the test while the simulated voltage changes significantly in amplitude between no-load and load.

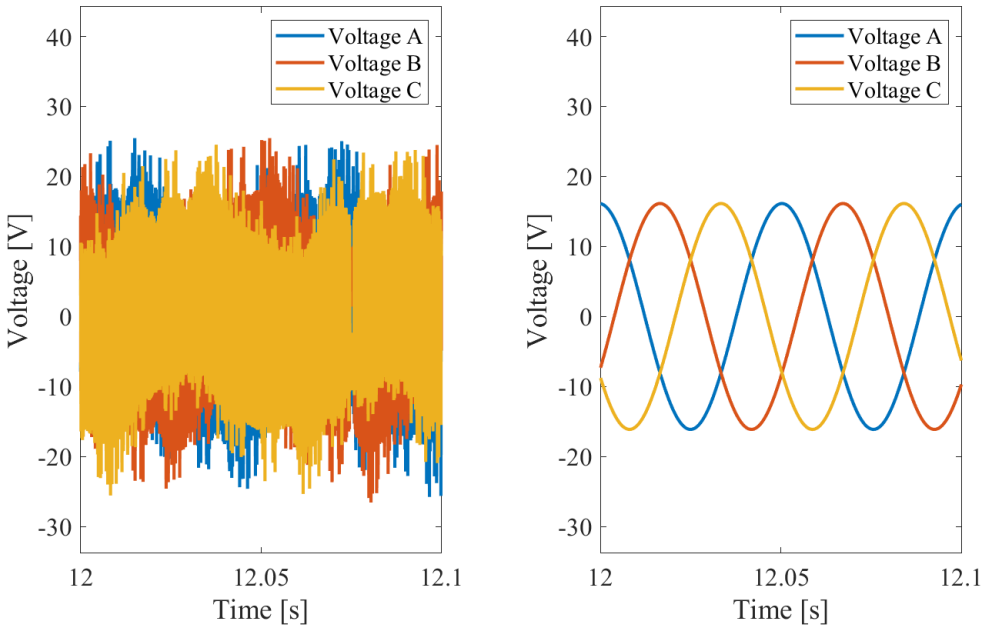

Figure 4.16: The measured (left) compared to the simulated (right) voltage test response zoomed in between 12 and 12.1 seconds of the test. There is a clear difference between the two graphs. The measured voltages shows that PWM signals have been used. The resulting voltage appears to be rougher and it is a bit difficult to distinguish the fundamental sine wave.

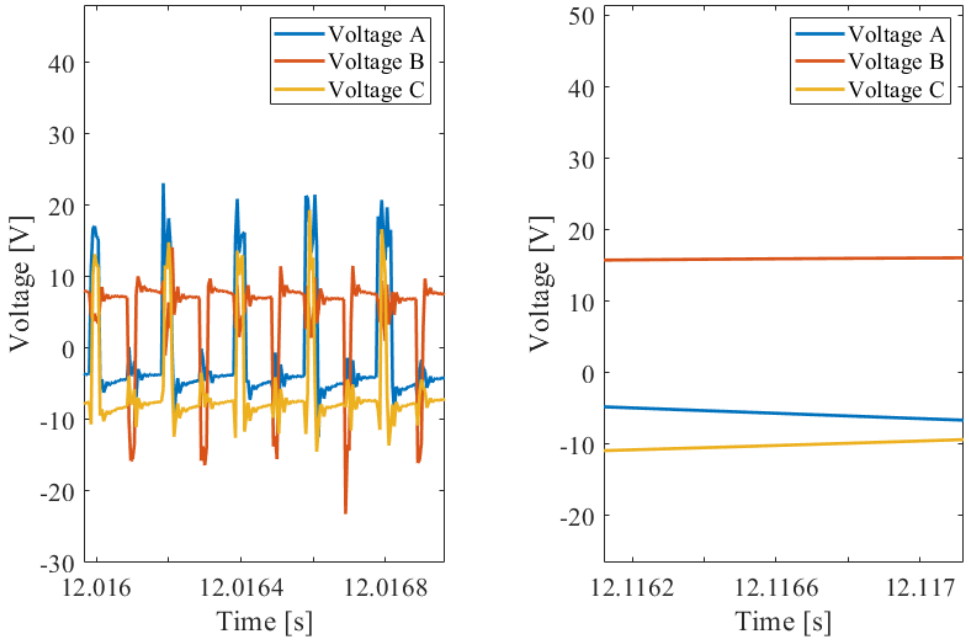

Figure 4.17: The measured (left) compared to the simulated (right) voltage test response zoomed in at a 1ms interval of the test. The difference in timings is because of small phase differences between the real and simulated results. The time intervals picked in this figure were chosen in order to make the measurements comparable (for visual purposes).

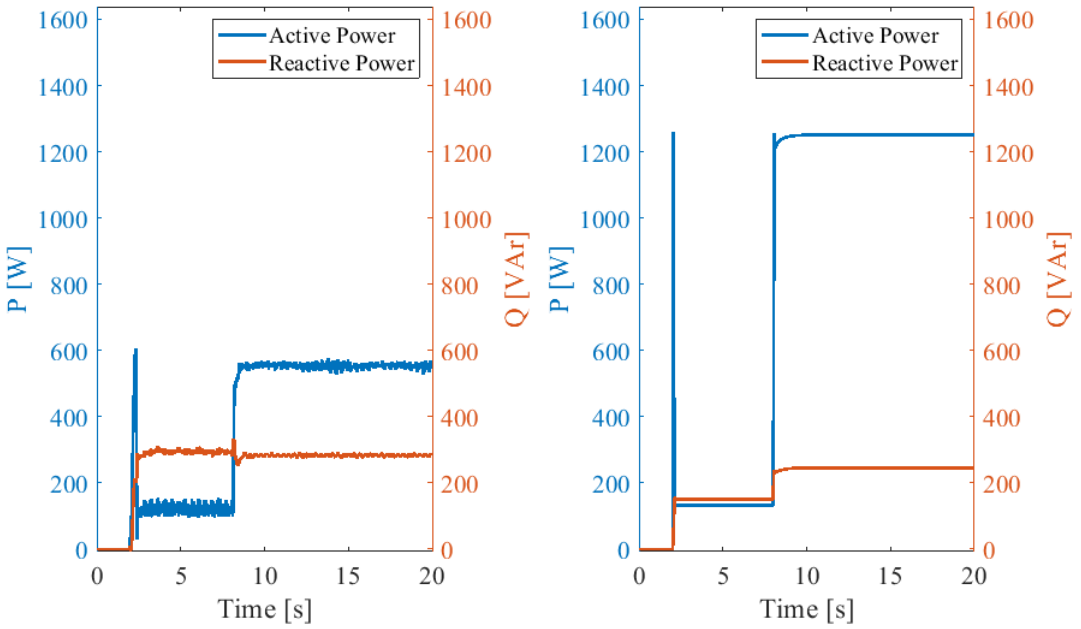

Figure 4.18: The measured (left) compared to the simulated (right) input active and reactive power. At no-load, reactive power is twice as large in the real machine compared to the simulation. Under load, the active input power in the simulated test is much higher than the input power in the test on the real machine.

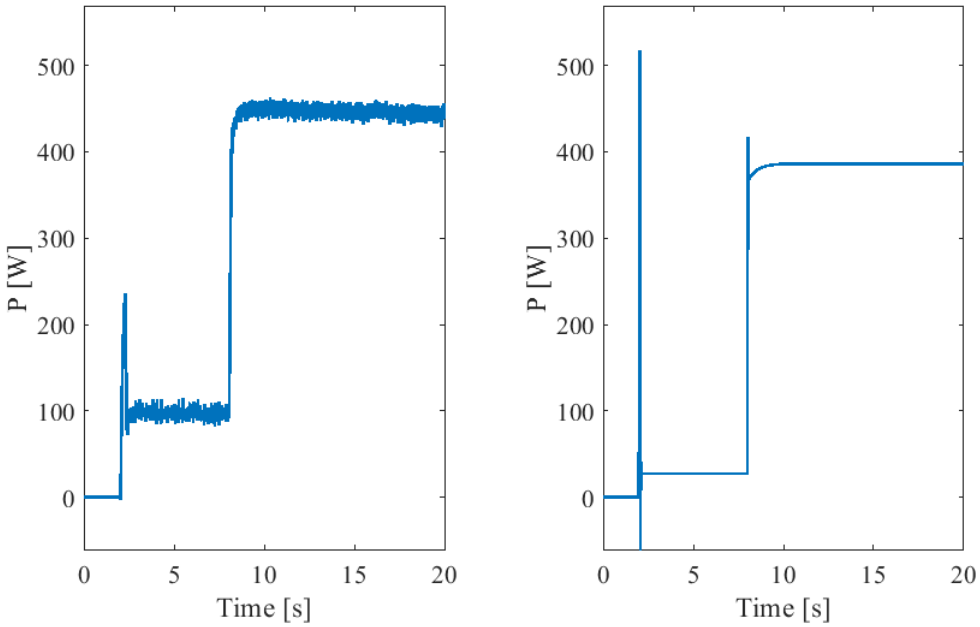

Figure 4.19: The measured (left) compared to the simulated (right) output active power. The simulated plot is more stable in steady state but has more oscillations in transient conditions. In no-load and during load the simulated output power was lower than for the real machine.

5
Discussion

In this chapter the results of the control programs and the results from the performance test on the large machine will be discussed. The ethical and environmental aspects of this project will also be discussed.

5.1 Control systems

5.1.1 Small machine

5.1.1.1 V/Hz

Since the flux in the machine was decided by the maximum voltage supplied to the machine and the base speed of the machine, the flux was severely weakened when the maximum supplied voltage was decreased to 60 V compared to the rated 230 V. This prompted the machine to not operate as requested since the flux was too low for operation at lower speeds. The conclusion from this was that the flux had to be artificially increased to the requested magnitude based on the rated voltage of the machine. This caused the machine to operate as expected for low speeds but it would enter flux weakening earlier based on the limited voltage that was provided.

5.1.1.2 FOC

In the simulations anti windup was not used in the beginning and it did not seem to be needed, but when the same control was tested in reality the problems became more visible. When the current controller was first tested on the small machine, the d-current would jump up to 1.6 A, which is approximately 1.6 Wb even though the requested flux was only 0.65 Wb. It would continue to hold this high d-current for about 20 seconds and then drop down to the correct requested value. The integrating regulator in the current regulator caused the delayed response. This required the controls to be improved with an anti windup, to prevent the integrating regulator from keeping high values for long periods of time. The saturation of the voltages was also improved so that the combined amplitude of the d and q voltages was limited instead of them both being limited separately.

When testing the current controller the small machine could initially only reach a speed of 350 rpm. This was caused by the high flux reference of 0.65 Wb. When running the previous versions of the FOC the flux was hovering at around 0.2 or

0.3 Wb when the reference was around 0.7 Wb. And, as expected, when the flux reference was lowered the machine was able to reach higher speed. The highest speed of around 1800 rpm was possible when using 0.13 Wb.

5.1.2 Large machine

5.1.2.1 V/Hz

The V/Hz control was the first control to be used on the large machine. It worked as it was supposed to and was able to make the machine rotate. The currents for low speeds were very high, which was expected due to the large V/Hz flux constant used in the program.

5.1.2.2 FOC

During the first testing of FOC on the large machine it was noted that the flux was weakened at around 350 rpm. The flux could not reach the flux reference of 0.1 Wb at this speed. This is because the DC-supply only supplies a maximum voltage of 30 V, which was limiting the available current supply. When the speed is increased the impedance of the motor will also increase due to the high inductance and their frequency dependency. The increasing impedance lowers the maximum current supply possible with the DC-supply used in the setup due to ohms law. This means that when 350 rpm is reached the rated maximum current of 95 A implemented in Simulink is not the real maximum output current with the current setup. This leads to that the controller asks for a higher current than the dc supply can deliver. The requested flux was therefore lowered to 0.04 Wb in order to achieve higher possible speeds.

The change of encoder when going from the setup for the small machine to the setup for the large machine introduced delay which caused instability. This was fixed with rearranging the connections and implementing frequency measurement between the encoder pulses instead of using the encoder block in Simulink. The new method of speed measurement increased measurement noise and therefore also caused some oscillations in the control. However, it was stable.

Overall the real measurements through the picoscope had noise, especially the torque. But the important ones are the currents and the speed which are a part of the feedback in the control. The often small but very fast and frequent oscillations and noise in the currents and speed feedback affect the regulators in the control. This influences the generation of voltage reference and in turn affects the switching signals sent to the inverter. Accurate measurement seems to be very important, especially when using a closed-loop control in real-time, if the goal is a stable control of an IM.

5.2 Performance test

In the results of the test on the large machine differences can be seen in all the plotted quantities. Just by quick examination it can be seen that the differences between measured and simulated speed and estimated rotor flux were quite low. However, the other plots of such as voltages, currents, torque and powers definitely did have some differences.

The torque ripple for the real machine was significant. To be able to view the torque the signal had to be processed with a moving average math function. The original signal was fluctuating between negative torque and positive torques during steady state operations. By using a moving average on the torque the resulting torque could be viewed. The resulting torque could be compared to the simulated torque and they were equivalent to each other. The simulated torque did not have this problem since it was stable during steady state operations.

The input power measured during the performance test was a lot lower than the simulated input power. It is hard to fully explain why this happened but something that probably contributed to this result was the inverter part. In the simulation the inverter was considered perfect, meaning that the requested and the resulting voltage after the inverter were identical. This is far from how the voltages after the inverter turned out in reality. Considering the differences it was probably not very realistic to assume a perfect inverter in the simulation.

The reactive and active power in the simulation seems to be too low during no-load, since during no-load operation the measured powers was approximately twice as large as the simulations.

A major factor contributing to differences between measured and simulated results could be noise in the measurements. As the field-oriented control program used for the test is a closed-loop system, the noise of measured feedback-values tend to affect the whole control. This probably created some unwanted small oscillations in all the measured quantities.

The accuracy of the simulation results could be affected by the accuracy of the estimated parameters and the fact that the mechanical damping constant B and the inertia constant J were guessed and not estimated. The parameters used for the control and simulation of the IM were the estimated values for 50 Hz, or 1500 rpm, operation, while the test only made the motor rotate with 500 rpm, which is translated to 16.7 Hz. This also leads to some small errors for the estimated parameters, which probably affected the results to some degree.

5.3 Sustainability, ethical and environmental perspective

Out of an environmental perspective this work can contribute both positively and negatively towards environmental sustainability. The purpose of this work is to progress towards more accurate and better simulation tools for induction machines. With better and more accurate tools one could argue that it is more likely that a good and efficient IM is easier made, which would be positive for the environment. But at the same time, better simulation tools could drive a trend towards making more and more machines which might be viewed as negative if this leads to overproduction.

For the ethical perspective of this work, this work can facilitate the implementation of cheaper and more efficient IMs in EVs. This can make EVs more affordable and accessible to a wider population, improving the living standards for many people. Long term increased efficiency and modelling of IM can help to decrease air-pollution as internal combustion engines can be replaced by electrical machines. Less air-pollution can in turn increase public health.

6
Conclusion

Conclusions from the work done in this project is presented here. Some ideas of further work that might be interesting to continue with in the future is also proposed.

6.1 Current work

6.1.1 Controllers

The control programs, V/Hz and FOC, created during this project required a lot of work. Towards the end of the work the controls functioned as intended.

6.1.1.1 V/Hz

V/Hz control is not suitable for situations where speed and torque needs to be controlled individually. It is not possible to keep requested speed when load is varied with this control system. Using a good flux proved to be very important for this controller.

6.1.1.2 FOC

FOC is complex and suitable for dynamic situations such as driving a car. It is important to keep the feedback measurements accurate to avoid introducing noise and oscillations into the controller. Correct methods for saturating currents and voltages to maximum values is important. Anti-windup was an important addition to keep regulators from keeping high reference values for extended periods of time. Anti-windup improved the response and stability of the FOC and was extra important for the real control.

6.1.2 The Performance test

6.1.2.1 Power

Differences can be seen between the measured and simulated tests regarding power however no full explanation to why these differences appear is included in this report due to the time limitation of the project.

6.1.2.2 Flux and Speed

The estimated rotor flux and speed were quite similar for the test.

6.1.2.3 Currents

For currents the main difference was more ripple for the measured currents in the real machine and some differences in amplitude between the real and simulated currents.

6.1.2.4 Voltages

Differences for voltages could be seen regarding the PWM pattern for the voltages in the real machine while the simulated voltages was perfect sine waves.

6.1.2.5 Torque

The torque for the real machine had large ripples during steady state meanwhile the simulated torque was stable.

6.1.3 Performance of the machine

One of the goals of this project was to evaluate the performance of the large machine, however this area was not fully investigated since there was not enough time in the end. It was also hard to do since there was a lot of unwanted noise and oscillations. During the performance test of the machine extra resistances was also present in the circuit. These resistances increased the losses of the machine.

6.2 Future work

During this project a lot of the time was spent on learning and creating the controls for the machines. Implementing the control system and making sure that the measured speed and currents could be used in the control system also took some effort. This led to that focus and time spent on analysing the machine and identifying the differences between measurement and simulation was somewhat decreased. In future projects it could be of interest to dig deeper in to why the simulations differ and how this can be resolved. It could also be interesting to further investigate the performance of the large machine. Identifying the parameters B and J for the large machine would also improve the comparisons for the performance test between the real and simulated machines.

Bibliography

[1] K. T. Chau, *Electric Vehicle Machines and Drives: Design, Analysis and Application*, Hong Kong, China: Wiley-IEEE Press, 2015. [Online]. Available: https://ieeexplore.ieee.org/book/7123280, Accessed on: 2024-06-03.

[2] L. Harnefors, *Control of Variable-Speed Drives*, Department of Electronics - Mälardalen University, Västerås, Sweden, 2002.

[3] S. Lundberg, *Electric Drive systems, Lecture 3 and 4*, Chalmers University of Technology, [Lecture slides]. 2024. Available: https://chalmers.instructure.com/courses/27791/files/3154570?module_item_id=442434

[4] M. Hinkkanen, *Lecture 2: V/Hz-Controlled Induction Motor Drive*, Aalto University, [Lecture slides]. 2023. Available: https://mycourses.aalto.fi/pluginfile.php/1955111/mod_resource/content/23/Lecture2.pdf

[5] S. Lundberg, *ENM076 Session 9: Field-Oriented control using internal flux sensors*, Chalmers University of Technology, [Lecture slides]. 2024. Available: https://chalmers.instructure.com/courses/27791/files/3220379?module_item_id=446046

[6] S. Lundberg, *Electric Drive systems, Lecture 10*, Chalmers University of Technology, [Lecture slides]. 2024. Available: https://chalmers.instructure.com/courses/27791/files/3256581?module_item_id=447467

[7] M. Hinkkanen, *Lecture 4: Pulse-Width Modulation and Current Control*, Aalto University, [Lecture slides]. 2024. Available: https://mycourses.aalto.fi/pluginfile.php/2226859/mod_resource/content/28/Lecture4.pdf

[8] Datasheet RI58-D 2020, Aldingen, Germany: Hengstler GMBH, 2020. [Online]. Available: https://www.hengstler.de/gfx/file/shop/encoder/RI58/datasheet_ri58-d_2020_en.pdf, Accessed on: 2024-04-20.

[9] Datasheet Torque Sensor DRBK + DRBK-A, Gschwend, Germany: ETH Messtechnik, 2023. [Online]. Available: https://www.eth-messtechnik.de/fileadmin/user_upload/engl._Datenblaetter_16.08.2023/DB003_DRBK-DRBK-A_EN_Rev.04.pdf, Accessed on: 2024-04-28.

A

Appendix

The figures in this Appendix is from the Matlab, Simulink programs that was used to simulate and control the induction machines.

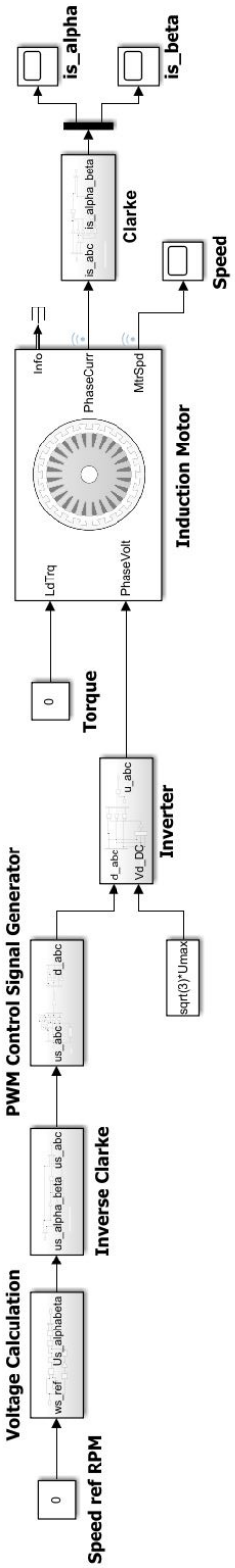

Figure A.1: The open-loop V/Hz controller for an Induction Machine in Simulink

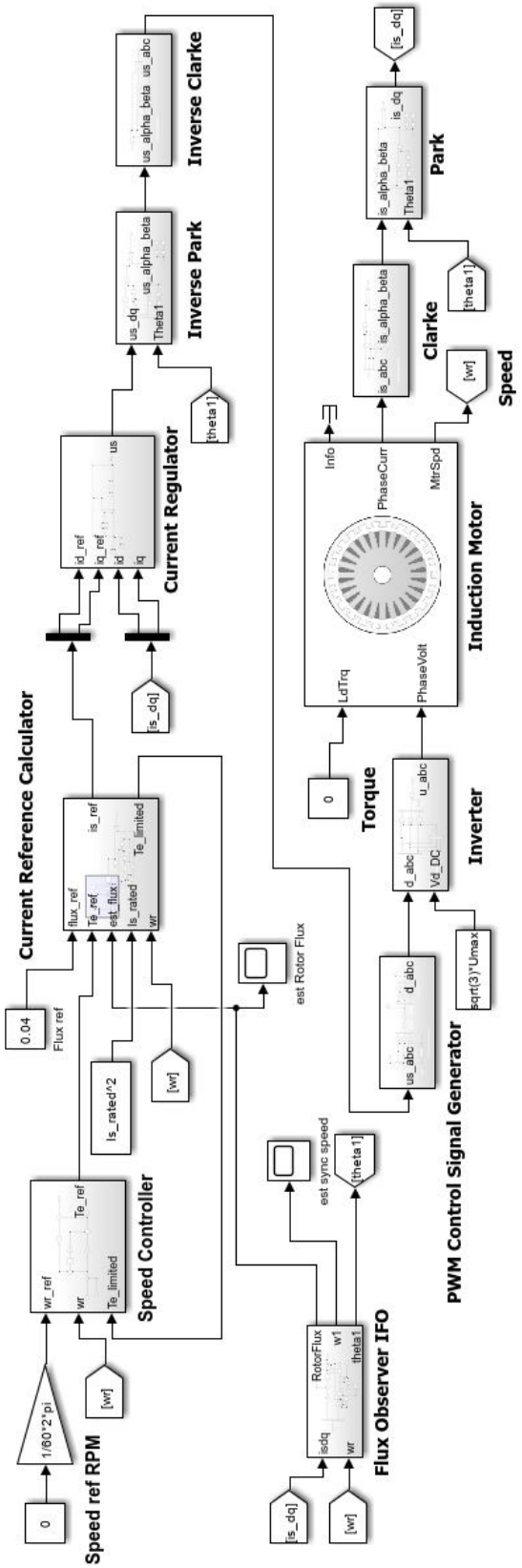

Figure A.2: FOC for a simulated Induction Machine in Simulink

DEPARTMENT OF ELECTRICAL ENGINEERING
CHALMERS UNIVERSITY OF TECHNOLOGY
Gothenburg, Sweden
www.chalmers.se

CHALMERS
UNIVERSITY OF TECHNOLOGY